

Mn(II) complexes of some acylhydrazones with NNO donor sites: Syntheses, a spectroscopic view on their coordination possibilities and crystal structures

Neema Ani Mangalam, S.R. Sheeja, M.R. Prathapachandra Kurup*

Department of Applied Chemistry, Cochin University of Science and Technology, Kochi, Kerala 682 022, India

ARTICLE INFO

Article history:

Received 12 March 2010

Accepted 7 September 2010

Available online 17 September 2010

Keywords:

Hydrazones
Crystal structures
Mn(II) complexes
EPR

ABSTRACT

Mn(II) complexes derived from a set of acylhydrazones were synthesised and characterized by elemental analyzes, IR, UV–vis and X-band EPR spectral studies as well as conductivity and magnetic susceptibility measurements. In the reported complexes, the hydrazones exist either in the keto or enolate form, as evidenced by IR spectral data. Crystal structures of two complexes are well established using single crystal X-ray diffraction studies. In both of these complexes two equivalent monoanionic ligands are coordinated in a meridional fashion using *cis* pyridyl, *trans* azomethine nitrogen and *cis* enolate oxygen atoms positioned very nearly perpendicular to each other. EPR spectra in DMF solutions at 77 K show hyperfine sextets and in some of the complexes the low intensity forbidden lines lying between each of the two hyperfine lines are also observed.

© 2010 Elsevier Ltd. All rights reserved.

1. Introduction

The coordination chemistry of transition metals with ligands from the hydrazine family has been of interest due to different bonding modes shown by them with both electron rich and electron poor metals. Acylhydrazones have been extensively investigated by chemists in the synthesis of coordination polymers owing to their inherent coordination and hydrogen-bonding donor/acceptor functionalities, as well as their biological activities [1,2]. Recently it was reported that such ligands, like non-symmetrical salens, can act as effective catalysts towards alkene epoxidation [3]. In analytical chemistry also, hydrazone ligands find wide applications as transition metal binders [4]. Studies have shown that the azomethine N, which has a lone pair of electrons in a sp^2 hybridized orbital, has considerable biological importance. Acylhydrazone complexes of transition metal ions are known to provide useful models for elucidation of the mechanism of enzyme inhibition by hydrazine derivatives and for their pharmacological applications [5]. Additionally hydrazone complexes have been the subject of studies over many years for their anti-bacterial and anti-tumor activities [6,7]. Manganese and its compounds find very historical importance in medicine and play a significant role in enzyme activation. It is well known that Mn plays an important role in many biological redox processes including disproportionation of H_2O_2 [8] (catalase activity) in microorganisms, decomposi-

tion of O_2^- radicals catalyzed by superoxide dismutases (SODs) and water oxidation by photosynthetic enzymes (photosystem II) [9,10].

This paper is an extension of our earlier studies with transition metal complexes of acylhydrazones [11,12]. An attractive aspect of hydrazones is that they are capable of exhibiting *keto-enol* tautomerism and can coordinate in tridentate neutral NNO donor mode [13], monoanionic NNO donor mode [14], dianionic tridentate ONO form [15], tetraanionic form [16] and bidentate neutral NO forms [17] to the metal ions generating mononuclear, dinuclear or polynuclear species. However, it depends on the reaction conditions, such as metal ion, its concentration, the pH of the medium and the nature of the hydrazone used. These interesting properties of the transition metal hydrazone complexes promoted us to synthesize Mn(II) complexes of some acylhydrazones and herein we report their syntheses, spectral characterization and crystal structures.

2. Experimental

2.1. Materials

2-Benzoylpyridine (Aldrich), di-2-pyridylketone (Aldrich), quinoline-2-carbaldehyde (Aldrich), benzhydrazide (Aldrich), and nicotinic hydrazide (Aldrich), manganese(II) acetate tetrahydrate (E-Merck), manganese(II) chloride tetrahydrate (E-Merck) were used as supplied and solvents were purified by standard procedure before use.

* Corresponding author. Tel.: +91 484 2862423; fax: +91 484 2575804.
E-mail address: mrp@cusat.ac.in (M.R.P. Kurup).

2.2. Syntheses of hydrazones

All the hydrazones were synthesised by the procedure reported by us earlier [11]. The hydrazones under investigation includes 2-benzoylpyridine benzoyl hydrazone (HBPB), di-2-pyridyl ketone nicotinoyl hydrazone (HDKN), quinoline-2-carbaldehyde benzoyl hydrazone (HQCB), quinoline-2-carbaldehyde nicotinoyl hydrazone (HQCN). The chemical structures and abbreviations for the ligands are given in Fig. 1.

2.3. Syntheses of complexes

2.3.1. Syntheses of $[Mn(BPB)_2]$ (**1**) and $[Mn(DKN)_2]$ (**2**)

To a solution of the appropriate acylhydrazone (1 mmol) in methanol one drop of triethylamine was added. To this, methanolic solution of $Mn(CH_3COO)_2 \cdot 4H_2O$ (1 mmol) was added and the reaction mixture was refluxed for 4 h. The resulting solution was allowed to stand at room temperature and after slow evaporation, brown crystalline product was separated, filtered and washed with ether and dried over P_4O_{10} *in vacuo*.

$[Mn(BPB)_2]$ (**1**): Yield: 85%, Color: brown, λ_m (DMF): $4 \Omega^{-1} cm^2 mol^{-1}$, μ_{eff} (B.M.): 5.48, Elemental Anal. Calc.: C, 69.62; H, 4.30; N, 12.82. Found: C, 69.56; H, 4.22; N, 12.48%.

$[Mn(DKN)_2]$ (**2**): Yield: 75%, Color: brown, λ_m (DMF): $7 \Omega^{-1} cm^2 mol^{-1}$, μ_{eff} (B.M.): 5.73, Elemental Anal. Calc.: C, 61.91; H, 3.67; N, 21.24. Found: C, 61.65; H, 3.61; N, 20.94%.

2.3.2. Syntheses of $[Mn(QCB)_2]$ (**3**) and $[Mn(QCN)_2]$ (**4**)

Complexes **3** and **4** were prepared in a similar manner as complexes **1** and **2** without adding triethylamine. The resulting solution was allowed to stand at room temperature and after slow evaporation, the dark blue compounds obtained were washed with methanol followed by ether and then dried over P_4O_{10} *in vacuo*.

$[Mn(QCB)_2]$ (**3**): Yield: 58%, Color: blue, λ_m (DMF): $8 \Omega^{-1} cm^2 mol^{-1}$, μ_{eff} (B.M.): 5.70, Elemental Anal. Calc.: C, 67.66; H, 4.01; N, 13.92. Found: C, 67.60; H, 4.41; N, 13.78%.

$[Mn(QCN)_2]$ (**4**): Yield: 54%, Color: blue, λ_m (DMF): $10 \Omega^{-1} cm^2 mol^{-1}$, μ_{eff} (B.M.): 5.91, Elemental Anal. Calc.: C, 63.47; H, 3.66; N, 18.51. Found: C, 63.57; H, 3.26; N, 18.30%.

2.3.3. Syntheses of $[Mn(HQCB)Cl_2]$ (**5**) and $[Mn(HQCN)Cl_2] \cdot 2H_2O$ (**6**)

Complexes **5** and **6** were prepared by refluxing equimolar methanolic solutions of appropriate acylhydrazone and $MnCl_2 \cdot 4H_2O$ for 4 h. and then kept at room temperature. The pale yellow compounds of **5** and **6** that separated out were filtered, washed with ether and dried over P_4O_{10} *in vacuo*.

$[Mn(HQCB)Cl_2]$ (**5**): Yield: 52%, Color: yellow, λ_m (DMF): $15 \Omega^{-1} cm^2 mol^{-1}$, μ_{eff} (B.M.): 6.13, Elemental Anal. Calc.: C, 50.90; H, 3.27; N, 10.47. Found: C, 50.24; H, 3.41; N, 10.53%.

$[Mn(HQCN)Cl_2] \cdot 2H_2O$ (**6**): Yield: 49%, Color: yellow, λ_m (DMF): $20 \Omega^{-1} cm^2 mol^{-1}$, μ_{eff} (B.M.): 5.67, Elemental Anal. Calc.: C, 43.86; H, 3.68; N, 12.79. Found: C, 44.27; H, 3.59; N, 12.93%.

2.4. Physical measurements

Elemental analyzes of the ligands and the complexes were performed on a Vario EL III CHNS analyzer at SAIF, Kochi, India. The IR spectra were recorded on a JASCO FT/IR-4100 Fourier Transform Infrared spectrometer using KBr pellets in the range 400–4000 cm^{-1} . The electronic spectral analyzes of ligands and their complexes were carried out in acetonitrile solution at room temperature on a Spectro UV–vis Double Beam UVD-3500 spectrometer in the 200–900 nm range. The molar conductances of the complexes in DMF (10^{-3} M) solutions were measured at 298 K with a Systronic model 303 direct-reading conductivity bridge. Magnetic susceptibility measurements for all the complexes

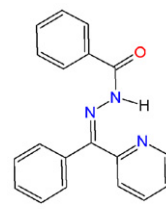
except **1** and **2** at room temperature were made using a Vibrating Sample Magnetometer at the Indian Institute of Technology, Roorkee, India and the other two were made using a MSB mk1 magnetic susceptibility balance from Sherwood Scientific Limited. EPR spectra of complexes in solid state at 298 K and in frozen DMF at 77 K were recorded on a Varian E-112 spectrometer at X-band, using TCNE as standard with 100 kHz modulation frequency and 9.1 GHz microwave frequency at SAIF, IIT Bombay, India.

2.5. X-ray crystallography

Small brown needle crystals of **1** ($0.20 \times 0.20 \times 0.30 mm^3$) were obtained by slow evaporation from its methanol–acetonitrile solution and the X-ray diffraction experiments were performed on a Bruker axis kappa apex2 CCD Diffractometer with graphite monochromated Mo $K\alpha$ radiation ($\lambda = 0.71073 \text{ \AA}$) at 293 K. The APEX2/SAINT and SAINT/XPREF softwares were used for cell refinement and data reduction, respectively. The structure was solved using SIR92 by direct method and refinement were carried out by the full matrix least squares method on F^2 using SHELXL-97. All non-hydrogen atoms were refined with anisotropic displacement parameters and the hydrogen atoms were placed at calculated positions and refined as riding atoms using isotropic displacement parameters.

Intensity data for a brown block shaped crystal of $[Mn(DKN)_2]$ ($0.10 \times 0.22 \times 0.32 mm^3$) grown from its methanolic solution was collected on a Bruker P4 X-ray diffractometer using graphite monochromated Mo $K\alpha$ radiation ($\lambda = 0.71073 \text{ \AA}$) at 293 K. The data were solved using SHELXL-97 [18] by direct method and each refinement was carried out by full-matrix least-squares on F^2 (SHELXL-97) with anisotropic displacement parameters for non-hydrogen atoms. The Bruker SAINT software was used for data reduction and Bruker SMART for cell refinement.

Crystal data and refinement details are given in Table 1 and molecular structure of $[Mn(BPB)_2]$ was drawn using the program DIAMOND version 3.1f [19] with 50% displacement ellipsoids.



HBPB

IR (KBr) cm^{-1} : $\nu(N-H)$ 3063; $\nu(C=O)$ 1678; $\nu(C=N)$ 1571.

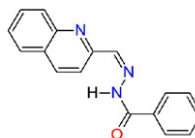
UV/vis (MeCN) λ_{max} (cm^{-1}): 42920, 36900, 31050.



HDKN

IR (KBr) cm^{-1} : $\nu(N-H)$ 2928; $\nu(C=O)$ 1689; $\nu(C=N)$ 1579.

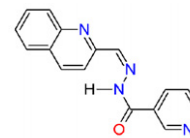
UV/vis (MeCN) λ_{max} (cm^{-1}): 44840, 37170, 31440.



HQCB

IR (KBr) cm^{-1} : $\nu(N-H)$ 3191; $\nu(C=O)$ 1655; $\nu(C=N)$ 1593.

UV/vis (MeCN) λ_{max} (cm^{-1}): 43790, 41640, 35860, 32580, 31690, 30430, 29130.



HQCEN

IR (KBr) cm^{-1} : $\nu(N-H)$ 3173; $\nu(C=O)$ 1656; $\nu(C=N)$ 1591.

UV/vis (MeCN) λ_{max} (cm^{-1}): 43920, 41490, 35840, 32580, 31750, 30440, 29150.

Fig. 1. Chemical structures of hydrazone ligands and their abbreviations.

3. Results and discussion

The synthesised hydrazones and complexes are very stable solids at room temperature without decomposition for a long time. As far as solubility is concerned, these hydrazones are fully soluble in most common organic solvents such as EtOH, MeOH, CHCl₃, CH₂Cl₂, etc. but the complexes have very low solubility and are only soluble in CH₃CN, DMF and DMSO. The Mn complexes synthesised were characterized by the analytical and spectroscopic techniques. In order to know further information about the coordi-

nation mode of the hydrazones, the IR spectra of their complexes were investigated and were found that ligands have coordinated either in neutral or monoanionic forms. Molar conductivity data reveal that the complexes are non-electrolytes, in accordance with the proposed formulations [20]. Magnetic measurements were recorded at room temperature for the complexes and their effective magnetic moment (μ_{eff}) values are given in Section 2.3. The magnetic moments of the Mn(II) complexes were observed in the range 5.48–6.13 B.M. [21] which are indicative of a high spin d⁵ system. After the syntheses of the complexes, we recrystallised **1** and **2** and

Table 1
Crystal data and structure refinement parameters for complexes **1** and **2**.

| Parameters | [Mn(BPB) ₂] (1) | [Mn(DKN) ₂] (2) |
|---|---|---|
| Empirical formula | C ₃₈ H ₂₈ MnN ₆ O ₂ | C ₃₄ H ₂₄ MnN ₁₀ O ₂ |
| Formula weight, <i>M</i> | 655.60 | 659.57 |
| Temperature, <i>T</i> (K) | 293(2) | 150 |
| Wavelength (Mo <i>K</i> α) (Å) | 0.71073 | 0.71073 |
| Crystal system | triclinic | monoclinic |
| Space group | <i>P</i> $\bar{1}$ | <i>P</i> 2 ₁ |
| <i>Lattice constants</i> | | |
| <i>a</i> (Å) | 10.4629(3) | 9.5069(7) |
| <i>c</i> (Å) | 12.6639(4) | 10.1525(7) |
| <i>b</i> (Å) | 13.2640(4) | 16.6511(10) |
| α (°) | 65.9150(10) | 90.00 |
| β (°) | 84.4190(10) | 100.390(7) |
| γ (°) | 84.9730(10) | 90.00 |
| Volume, <i>V</i> (Å ³) | 1594.66(8) | 1580.79(19) |
| <i>Z</i> | 2 | 2 |
| Calculated density, ρ (Mg m ⁻³) | 1.365 | 1.386 |
| Absorption coefficient, μ (mm ⁻¹) | 0.459 | 0.466 |
| Limiting indices | –15 ≤ <i>h</i> ≤ 15 –18 ≤ <i>k</i> ≤ 18 –19 ≤ <i>l</i> ≤ 19 | –11 ≤ <i>h</i> ≤ 11 –11 ≤ <i>k</i> ≤ 11 –19 ≤ <i>l</i> ≤ 19 |
| Reflections collected (<i>R</i> _{int}) | 44 066 (0.0398) | 11 389 (0.0240) |
| Unique reflections | 10 915 | 5359 |
| Refinement method | full-matrix least-squares on <i>F</i> ² | full-matrix least-squares on <i>F</i> ² |
| Data/restraints/parameters | 10915/0/425 | 5359/1/425 |
| Goodness-of-fit on <i>F</i> ² | 0.998 | 1.046 |
| Final <i>R</i> indices [<i>I</i> > 2σ(<i>I</i>)] | <i>R</i> ₁ = 0.0479, <i>wR</i> ₂ = 0.1207 | <i>R</i> ₁ = 0.0438, <i>wR</i> ₂ = 0.1243 |
| <i>R</i> indices (all data) | <i>R</i> ₁ = 0.1092, <i>wR</i> ₂ = 0.1571 | <i>R</i> ₁ = 0.0514, <i>wR</i> ₂ = 0.1277 |

$$wR_2 = [\sum w(F_o^2 - F_c^2)^2 / \sum w(F_o^2)^2]^{1/2}$$

$$R_1 = \sum ||F_o| - |F_c|| / \sum |F_o|$$

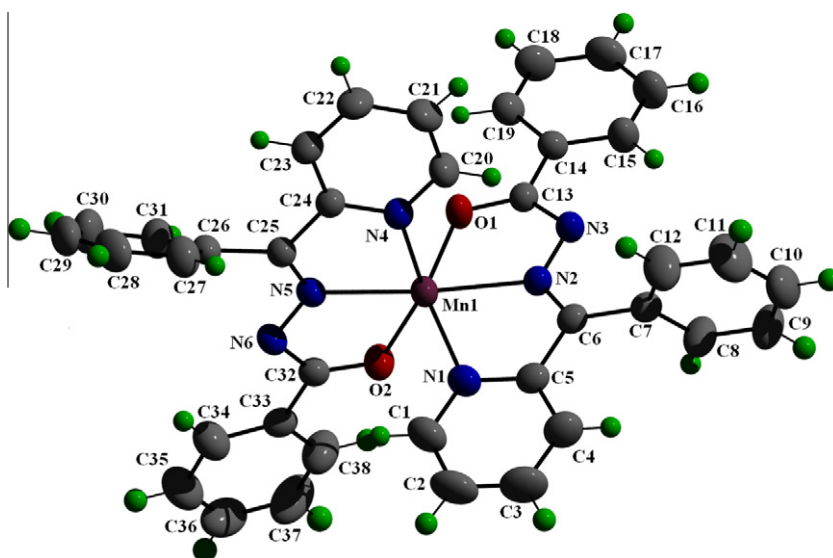


Fig. 2. Molecular structure of [Mn(BPB)₂] (**1**) along with the atom numbering scheme (displacement ellipsoids are drawn at the 50% probability level and hydrogen atoms are shown as small spheres of arbitrary radii).

obtained suitable single crystals for X-ray diffraction analyzes. From the crystal structures it was found that in both cases the ligands HBPB and HDKN coordinate via pyridyl, azomethine nitrogens and enolate oxygens.

Table 2
Selected bond lengths (Å) and bond angles (°) for HBPB, complexes **1** and **2**.

| | HBPB | [Mn(BPB) ₂] (1) | [Mn(DKN) ₂] (2) |
|-----------|-----------|--------------------------------------|--------------------------------------|
| Mn1–N2 | – | 2.190(2) | Mn1–N3 2.204(3) |
| Mn1–N5 | – | 2.194(2) | Mn1–N8 2.195(3) |
| Mn1–O1 | – | 2.120(1) | Mn1–O1 2.133(3) |
| Mn1–O2 | – | 2.096(1) | Mn1–O2 2.125(3) |
| Mn1–N1 | – | 2.287(2) | Mn1–N1 2.313(3) |
| Mn1–N4 | – | 2.284(2) | Mn1–N6 2.268(3) |
| N2–N3 | 1.3682(2) | 1.369(2) | N3–N4 1.375(4) |
| N5–N6 | – | 1.370(2) | N8–N9 1.373(4) |
| N2–C6 | 1.2955(2) | 1.287(2) | N3–C6 1.280(5) |
| N5–C25 | – | 1.292(2) | N8–C23 1.295(5) |
| C13–O1 | 1.2213(1) | 1.267(2) | C12–O1 1.261(4) |
| N3–C13 | 1.3610(2) | 1.332(2) | N4–C12 1.343(5) |
| N6–C32 | – | 1.334(2) | N9–C29 1.326(5) |
| O1–C13–N3 | 124.67(1) | 125.97(2) | O1–C12–N4 126.80(3) |
| N2–Mn1–N5 | – | 164.16(5) | N3–Mn1–N8 161.95(1) |
| N2–Mn1–O1 | – | 71.75(5) | N3–Mn1–O1 72.41(1) |
| N1–Mn1–N4 | – | 97.76(6) | N1–Mn1–N6 97.38(1) |
| N5–Mn1–O2 | – | 71.75(5) | N8–Mn1–O2 72.15(1) |
| N1–Mn1–N2 | – | 71.14(5) | N1–Mn1–N3 71.23(1) |
| N4–Mn1–N5 | – | 71.33(5) | N6–Mn1–N8 70.85(1) |
| O1–Mn1–O2 | – | 101.40(5) | O1–Mn1–O2 102.48(1) |
| O1–Mn1–N1 | – | 142.04(5) | O1–Mn1–N1 143.59(1) |
| O2–Mn1–N4 | – | 143.07(5) | O2–Mn1–N6 142.15(1) |
| N2–Mn1–N4 | – | 94.19(5) | N3–Mn1–N6 96.48(1) |
| N5–Mn1–N1 | – | 103.69(6) | N8–Mn1–N1 97.08(1) |
| C6–N2–N3 | 117.38(1) | 120.01(1) | C6–N3–N4 120.20(3) |
| N2–C6–C5 | 127.69(1) | 114.57(2) | N3–C6–C5 115.10(3) |
| N2–C6–C7 | 114.35(1) | 125.26(2) | N3–C6–C7 125.50(3) |

Table 3
H-bonding, π – π and C–H... π interaction parameters in [Mn(BPB)₂] and [Mn(DKN)₂].

| | | | | |
|--|------------|-------|--------------|-------------|
| <i>[Mn(BPB)₂]</i> | | | | |
| H-bonding interactions | | | | |
| D–H...A (Å) | D–H | H...A | D...A | D–H...A (°) |
| C8–H(8)...N(3) ^a | 0.93 | 2.57 | 3.332 | 140 |
| Equivalent position code | | | | |
| a = 1 – x, 1 – y, 2 – z | | | | |
| π – π interactions | | | | |
| Cg(I)...Cg(J) | Cg–Cg (Å) | | α (°) | β (°) |
| Cg(6)...Cg(6) ^b | 3.731 | | 0.03 | 18.63 |
| Equivalent position code | | | | |
| b = 2 – x, –y, 2 – z | | | | |
| C–H... π interaction | | | | |
| X–H...Cg(J) | H...Cg (Å) | | X–H...Cg (°) | X...Cg (Å) |
| C(9)–H(9)...Cg(1) ^c | 2.74 | | 139 | 3.492 |
| Equivalent position code | | | | |
| c = 1 – x, 1 – y, 2 – z | | | | |
| <i>[Mn(DKN)₂]</i> | | | | |
| H-bonding interactions | | | | |
| D–H...A (Å) | D–H | H...A | D...A | D–H...A (°) |
| C16–H(16)...N(4) ^d | 0.93 | 2.60 | 3.523 | 176 |
| Equivalent position code | | | | |
| d = –x, –1/2 + y, –z | | | | |
| π – π interactions | | | | |
| Cg(I)...Cg(J) | Cg–Cg (Å) | | α (°) | β (°) |
| Cg(1)...Cg(6) ^e | 3.751 | | 17.49 | 13.44 |
| Equivalent position code | | | | |
| e = 1 – x, –1/2 + y, –z | | | | |
| C–H... π interaction | | | | |
| X–H...Cg(J) | H...Cg (Å) | | X–H...Cg (°) | X...Cg (Å) |
| C(28)–H(28)...Cg(2) ^f | 2.65 | | 146 | 3.462 |
| Equivalent position code | | | | |
| f = 1 – x, 1/2 + y, 1 – z | | | | |
| Cg(2) = Mn(1), O(2), C(29), N(9), N(8) | | | | |

D, donor; A, acceptor; Cg, centroid; α , dihedral angles between planes I and J; β , angle Cg(1)–Cg(J) vector and normal to plane I.

3.1. Crystal structures of [Mn(BPB)₂] (**1**) and [Mn(DKN)₂] (**2**)

The manganese atom in [Mn(BPB)₂] and [Mn(DKN)₂] is coordinated in a distorted octahedral arrangement in which each ligand binds as a monoanionic N,N,O chelator in a meridional fashion. A perspective view of **1** along with the atom numbering scheme is depicted in Fig. 2 and relevant bond lengths and angles of **1** and **2** are listed in Table 2. The coordinated ligands form two five membered chelate rings, imposing large distortions on the ideally octahedral coordinate angles. The *trans* angle N2–Mn–N5 and N3–Mn1–N8 is much farther from 180°, 164.16(5)° in **1** and 161.95(11)° and **2**, respectively, compared with similar Cu (178.03°) and Zn (175.23°) complexes [22], whereas the *trans* N1–Mn–O1 (142.04(5)°) and N4–Mn–O2 (143.07(5)°) angles in **1** defined by each meridionally coordinated ligand also deviate markedly from linearity. The intraligand bite angles are correspondingly more acute at ~71.49° in **1** and ~71.66° in **2** when compared to other metal complexes reported with similar ligands. As the coordinate bonds become longer, the inflexible ligand maintains the same conformation, leading to the contraction of the coordinate angles. The crystal structure of HBPB was reported by us earlier [11] and although the C6–N2 and N2–N3 bond lengths are less affected by the complexation [ca. 1.287 and 1.369 Å in complex compared with 1.295 and 1.368 Å in free ligand, respectively], the C13–O1 bond lengths significantly (by ca. 0.04 Å). Relevant bond length and bond angles of HBPB [11] are tabulated in Table 2. Overall, these observations are consistent with the enolate resonance form of HBPB being dominant in the deprotonated coordinated ligand, and this is supported by the IR spectral data. In **2** as a consequence of deprotonation, the C13–O1 and C32–O2 bonds lengthen and the negative charge of the monoanionic ligand is delocalized over the DKN moiety. Both the bicyclic chelate rings are close to being

perpendicular to each other with a dihedral angle of 86.24° and 86.13° in **1** and **2**, respectively. The M–N_(pyridine), M–N_(imine) and M–O bond lengths observed here are within the range reported for other similar complexes of divalent metal ions [23,24].

No classical hydrogen bond was found in the crystal structure of **1**. The crystal packing is determined by intermolecular hydrogen bonds, π – π interactions and C–H... π interactions (Table 3). In the crystal structure of **2**, the asymmetric units are linked by intermolecular interactions (Table 3) and gives stability to the complex.

3.2. Infrared spectra

The significant IR frequencies of the ligands are shown in Fig. 1. The main stretching frequencies of the IR spectra of the complexes and their tentative assignments are tabulated (see Supplementary material). Comparing the IR spectra of the ligands with that of the complexes, we observed that $\nu(\text{NH})$ and $\nu(\text{C}=\text{O})$ stretching vibrations of the ligands disappeared in the IR spectra of their complexes except in **5** and **6**, which showed that the frame H–N–C=O has transformed to N=C–O–H form coordinating to metal (Mn) in *enolate* form [25]. Additionally a new C–O absorption band appeared in the range 1348–1368 cm^{-1} in all the complexes except **5** and **6**. Both of the $\nu(\text{NH})$ and $\nu(\text{C}=\text{O})$ bands were retained in the metal complexes **5** and **6** but were shifted towards lower frequencies, indicating that the hydrazone ligand has not undergone enolization but has coordinated to the metal center in *keto* form [26]. The $\nu(\text{C}=\text{N})$ stretching bands are strongly affected by chelation and shifted to lower wavenumbers which is attributed to the conjuga-

tion of the p-orbital on the double bond with the d-orbital on the metal ion with the reduction of the force constant [27]. This supports the participation of imine group of these ligands in binding to the metal ion. The appearance of a new band due to the new $\nu(\text{C}=\text{N})$ formed as a result of enolization of the ligands at $\sim 1585 \text{ cm}^{-1}$ may be taken as additional evidence for the participation of the imine nitrogen in coordination [28]. The low energy pyridine ring out-of-plane vibrations observed in the spectra of ligands at $\sim 650 \text{ cm}^{-1}$ are shifted to higher frequencies in the case of complexes, which are good indication of the coordination of the heterocyclic nitrogen atom. The ligand coordination is substantiated by two bands appearing at $\sim 487, 436 \text{ cm}^{-1}$ for the complexes; these are mainly attributed to $\nu(\text{M}-\text{N})$ and $\nu(\text{M}-\text{O})$, respectively. The far IR spectra of the complexes **5** and **6** display peaks at 303 and 321 cm^{-1} indicating the terminal coordination of chlorine atom [29]. From the above observations it was found that the hydrazones under study could coordinate both in keto and in enolate form.

3.3. Electronic and EPR spectra

The absorption bands of the ligands are shown in Fig. 1 and that of complexes are tabulated (see Supplementary material). The ground state of high-spin octahedral Mn(II) complex is ${}^6\text{A}_{1\text{g}}$ and as there are no excited terms of sextet spin multiplicity, d–d transitions are doubly forbidden. However, some forbidden transitions occur and consequently, these transitions have an extremely low molar extinction coefficient value. The electronic spectra of the manganese(II) complexes exhibit four weak intensity absorption bands in the ranges 17 280–18 950; 23 923–28 380; 28 450–28 980; 31 055–31 600 cm^{-1} , which may be assigned to the transitions: ${}^4\text{T}_{1\text{g}}({}^4\text{G}) \leftarrow {}^6\text{A}_{1\text{g}}$, ${}^4\text{A}_{1\text{g}}({}^4\text{G})$, ${}^4\text{E}_{\text{g}} \leftarrow {}^6\text{A}_{1\text{g}}$, ${}^4\text{E}_{\text{g}}({}^4\text{D}) \leftarrow {}^6\text{A}_{1\text{g}}$, ${}^4\text{T}_{1\text{g}}({}^4\text{P}) \leftarrow {}^6\text{A}_{1\text{g}}$, respectively. For octahedral Mn(II) complexes, electronic spectra normally show two bands ca. 18 000 and 20 000 cm^{-1} , which are assigned to ${}^4\text{T}_{1\text{g}}(\text{G}) \leftarrow {}^6\text{A}_{1\text{g}}$ and ${}^4\text{T}_{2\text{g}}(\text{G}) \leftarrow {}^6\text{A}_{1\text{g}}$, respectively [30]. But the high intense charge transition tailing into the visible region, obscure the very weak d–d absorptions of the Mn(II) complexes.

The electron spin properties of manganese have long been of interest as a spectroscopic probe of manganese centers in manganese proteins. The Mn(II) oxidation state possesses Kramers' ground-state doublets and exhibits characteristic spin transitions in the normal mode X-band regime. The spin Hamiltonian,

$$\hat{H} = g\beta BS + IAS + D \left[S_z^2 - \frac{S(S+1)}{3} \right] + E(S_x^2 - S_y^2)$$

where B is the magnetic field vector, g is the spectroscopic splitting factor, β is the Bohr magneton, D is the axial zero field splitting parameter, E is rhombic zero field splitting parameter and S is the electron spin vector. The first two terms represent the electronic Zeeman and the electron nuclear hyperfine interactions, respectively, whereas the last two terms define the zero-field splitting interaction with D and E gauging the axial and the rhombic parts.

Mn^{2+} (d^5) being an odd electron system, the zero-field splitting produces three doubly degenerate spin states $M_s = \pm 5/2, \pm 3/2, \pm 1/2$ (Kramers' degeneracy). Each of these is split into two singlets by the applied field, producing six levels. As a result of this splitting, five transitions ($-5/2 \rightarrow -3/2, -3/2 \rightarrow -1/2, -1/2 \rightarrow 1/2, 1/2 \rightarrow 3/2, 3/2 \rightarrow 5/2$) are expected. But in practice usually only one signal is observed since they are of equal energy. The spectrum will further split by the nuclear hyperfine interaction with the Mn nucleus ($I = 5/2$) which would give rise to thirty peaks in the spectrum.

EPR spectra of $[\text{Mn}(\text{DKN})_2]$ and $[\text{Mn}(\text{HQCN})\text{Cl}_2] \cdot 2\text{H}_2\text{O}$ in polycrystalline state at 298 K gave a broad signal with $g = 2.083$ and

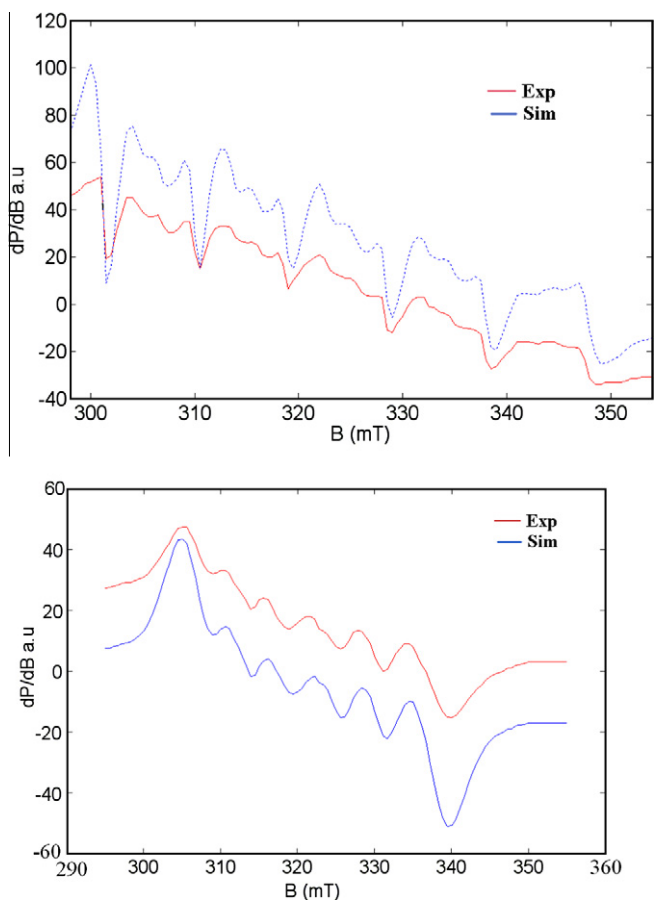


Fig. 3. Simulated and experimental best fits of EPR spectra of $[\text{Mn}(\text{DKN})_2]$ (above) and $[\text{Mn}(\text{HQCB})\text{Cl}_2]$ (below) in frozen DMF at 77 K.

2.053, respectively, without any resolved hyperfine splitting. The broadness of the spectra may be due to immobilization of Mn(II) ion in the complex or may be due to dipolar interactions and enhanced spin lattice relaxation. However, when recorded in DMF at 77 K, both spectra exhibit sixfold well-resolved hyperfine splitting pattern with hyperfine coupling constants 9.3 and 8.97 mT, respectively, arising due to the hyperfine interaction between the unpaired electron with the ^{55}Mn nucleus ($I = 5/2$) [31]. The frozen solution spectrum of **2** and **5** in DMF at 77 K was simulated using EasySpin [32]. The observed g values are very close to the free electron spin value of 2.0023 which is consistent with the typical Mn(II) and also suggestive of the absence of spin orbit coupling in the ground state ${}^6\text{A}_{1g}$ without another sextet term of higher energy. In addition to this, a pair of low intensity lines is found in between each of the two main hyperfine levels (Fig. 3). These are the forbidden lines with an average spacing of ~ 2.5 mT corresponding to $\Delta m_l = \pm 1$ transitions arising due to the mixing of hyperfine lines with zero field splitting [33]. For the complex **2**, axial splitting factor D , rhombic splitting factor E and E/D ratio were found to be 420, 120 MHz and 0.285, respectively.

In the case of $[\text{Mn}(\text{BPB})_2]$ and $[\text{Mn}(\text{HQCBCl}_2)_2]$ in polycrystalline state at 298 K two signals were observed with two g values with no hyperfine splittings. The frozen solution spectrum of **1** in DMF at 77 K also displayed two signals with g values; $g_1 = 2.091$ and $g_2 = 4.999$ in which one signal showed hyperfine sextet with hyperfine coupling constant 7.7 mT. In the case of **5**, when recorded in DMF at 77 K the compound displayed only one signal with sixfold hyperfine splitting pattern corresponding to $\Delta M_s = \pm 1$ transitions with hyperfine coupling constant 6.0 mT (Fig. 3). The forbidden lines in the spectrum of **1** arise due to the mixing of the nuclear hyperfine levels by the zero field splitting factor of the Hamiltonian. EPR spectra of $[\text{Mn}(\text{QCB})_2]$ in polycrystalline state at 298 K and in frozen DMF exhibit three signals. The three g values imply that the molecule is rhombically distorted. The compound $[\text{Mn}(\text{QCN})_2]$ in polycrystalline state at 298 K gave two broad signals with no hyperfine splitting and in DMF at 77 K the compound displayed four signals in which one of the signal displayed a hyperfine sextet.

Acknowledgments

M.R.P. Kurup is thankful to KSCSTE, Thiruvananthapuram, India for financial assistance and N.A. Mangalam thanks the Cochin University of Science and Technology for the award of Senior Research Fellowship. S.R.S. thanks CSIR, New Delhi for the award of Senior Research Fellowship. The authors are thankful to the SAIF, Cochin University of Science and Technology, Kochi, Kerala, India for elemental and IR analyses. We are thankful to IIT Bombay, India for EPR spectra. We also thank Prof. M.V. Rajasekharan, School of Chemistry, University of Hyderabad and Dr. Babu Varghese, SAIF, IIT Madras for providing single crystal XRD data.

Appendix A. Supplementary data

CCDC 715900 and 767043 contain the supplementary crystallographic data for compounds $[\text{Mn}(\text{BPB})_2]$ and $[\text{Mn}(\text{DKN})_2]$. These data can be obtained free of charge via <http://www.ccdc.cam.ac.uk/conts/retrieving.html>, or from the Cambridge Crystallographic Data Centre, 12 Union Road, Cambridge CB2 1EZ, UK; fax: +44 1223 336 033; or e-mail: deposit@ccdc.cam.ac.uk. Supplementary data associated with this article can be found, in the online version, at doi:10.1016/j.poly.2010.09.007.

References

- [1] S. Dutta, V. Manivannan, L.G. Babu, S. Pal, Acta Crystallogr., Sect. C 51 (1995) 813.
- [2] Z.-X. Lian, P. Liu, J.-M. Zhang, T.-J. Lou, T.-X. Wang, H.-H. Li, Chin. J. Struct. Chem. 27 (2008) 639.
- [3] O. Pouralimardan, A.-C. Chamayou, C. Janiak, H.H. Monfared, Inorg. Chim. Acta 360 (2007) 1599.
- [4] M. Katyal, Y. Dutt, Talanta 22 (1975) 151.
- [5] J.D. Dilworth, Coord. Chem. Rev. 21 (1976) 29.
- [6] U.O. Ozmen, G. Olgun, Spectrochim. Acta, Part A 70 (2008) 641.
- [7] P.V. Bernhardt, J. Mattson, Des R. Richardson, Inorg. Chem. 45 (2006) 752.
- [8] M. Pick, I. Roboni, J. Fridovich, J. Am. Chem. Soc. 96 (1974) 7329.
- [9] R.J. Debus, Biochim. Biophys. Acta 1102 (1992) 269.
- [10] G. Christou, J.B. Vincent, Inorg. Chim. Acta 136 (1987) L41.
- [11] N.A. Mangalam, S. Sivakumar, S.R. Sheeja, M.R.P. Kurup, E.R.T. Tiekink, Inorg. Chim. Acta 362 (2009) 4191.
- [12] N.A. Mangalam, S. Sivakumar, M.R.P. Kurup, Spectrochim. Acta, Part A 75 (2010) 686.
- [13] A.A.R. Despaigne, J.G. Da Silva, A.C.M. Do Carmo, O.E. Piro, E.E. Castellano, H. Beraldo, Inorg. Chim. Acta 362 (2009) 2117.
- [14] S. Koner, S. Saha, T. Mallah, K. Okamoto, Inorg. Chem. 43 (2004) 840.
- [15] E.B. Seenaa, N. Mathew, M. Kuriakose, M.R.P. Kurup, Polyhedron 27 (2008) 1455.
- [16] J. Chakraborty, S. Thakurta, G. Pilet, D. Luneau, S. Mitra, Polyhedron 28 (2009) 819.
- [17] S. Banerjee, A. Ray, S. Sen, S. Mitra, D.L. Hughes, R.J. Butcher, S.R. Batten, D.R. Turner, Inorg. Chim. Acta 361 (2008) 2692.
- [18] G.M. Sheldrick, SHELXS97 and SHELXL97, Bruker AXS Inc., Madison, WI, USA, 1999.
- [19] K. Brandenburg, DIAMOND Version 3.1f, Crystal Impact GbR, Bonn, Germany, 2008.
- [20] W.J. Geary, Coord. Chem. Rev. 7 (1971) 109.
- [21] P.F. Rapheal, E. Manoj, M.R.P. Kurup, Polyhedron 26 (2007) 5088.
- [22] C.M. Armstrong, P.V. Benhardt, P. Chin, Des R. Richardson, Eur. J. Inorg. Chem. (2003) 1145.
- [23] A. Ray, S. Banerjee, S. Sen, R.J. Butcher, G.M. Rosair, M.T. Garland, S. Mitra, Struct. Chem. 19 (2008) 209.
- [24] A.R. Stefankiewicz, M.W. Chorab, H.B. Szczesniak, V. Patroniak, M. Kubicki, Z. Hnatejko, J. Harrowfield, Polyhedron 29 (2009) 178.
- [25] Cao-Y. Meng, Xin-S. Wan, Xian-F. Zheng, Lu-Y. Meng, Hong-Y. Zhang, R. Yang, Hong-W. Hou, Synth. React. Inorg. Met. Org. Nano Met. Chem. 37 (2007) 97.
- [26] S.A. El-Enein, F.A. El-Saied, S.M. Emam, M.A. Ell-Salamony, Spectrochim. Acta, Part A 71 (2008) 421.
- [27] M. Aslantas, E. Kendi, N. Demir, A.E. Sabik, M. Tumer, M. Kertmen, Spectrochim. Acta, Part A 74 (2009) 617.
- [28] X.-H. Chen, Q.-J. Wu, Z.-Y. Liang, C.-R. Zhan, J.-B. Liu, Acta Crystallogr., Sect. C 65 (2009) 190.
- [29] V. Philip, V. Suni, M.R.P. Kurup, M. Nethaji, Polyhedron 25 (2006) 1931.
- [30] M.S. Refat, S. Chandra, M. Tyagi, J. Therm. Anal. Calorim. 100 (2009) 261.
- [31] R. Kumar, S. Chandra, Spectrochim. Acta, Part A 67 (2007) 188.
- [32] S. Stoll, A. Schweiger, J. Magn. Reson. 178 (2006) 42.
- [33] T.H. Bennur, D. Srinivas, P. Ratnasamy, Microporous Mesoporous Mater. 48 (2001) 111.